

<https://doi.org/10.1038/s43247-024-01346-2>

Record-breaking fire weather in North America in 2021 was initiated by the Pacific northwest heat dome

Check for updates

Piyush Jain ¹✉, Aseem Raj Sharma², Dante Castellanos Acuna³, John T. Abatzoglou ⁴ & Mike Flannigan⁵

The 2021 North American wildfire season was marked by record breaking fire-conducive weather and widespread synchronous burning, extreme fire behaviour, smoke and evacuations. Relative to 1979–2021, the greatest number of temperature and vapor pressure deficit records were broken in 2021, and in July alone, 3.2 million hectares burned in Canada and the United States. These events were catalyzed by an intense heat dome that formed in late June over western North America that synchronized fire danger, challenging fire suppression efforts. Based on analysis of persistent positive anomalies of geopotential heights, the heat dome accounted for 21–34% of the total area burned in 2021. The event was 59% longer, 34% larger and had 6% higher maximum amplitude than the same event would have been without a warming climate. Climate change will continue to magnify heat dome events, increase fire danger, and enable extreme synchronous wildfire in forested areas of North America.

One of the main weather stories of 2021 was the extraordinary heatwave that started in late June in the Pacific Northwest, leading to extreme temperatures in British Columbia, Washington and Oregon; this event led to the small town of Lytton, British Columbia experiencing the highest ever recorded temperature in Canada with 49.6 °C on June 29th with a subsequent wildfire that destroyed the town¹. The British Columbia Coroner's Office confirmed 619 heat-related deaths during the most intense period of the heatwave (June 25–July 1²) with significant heat-related fatalities also recorded during the same period in the states of Oregon³ and Washington⁴. Observed surface temperature anomalies during the heatwave were extremely rare exceeding $4.5 \sigma^5$, found to be one of the most extreme heatwaves globally⁶, and was estimated as a one-in-a-thousand-year event that would have been 150 times less likely without climate change⁷. The 2021 Pacific Northwest heatwave has been popularly referred to as a heat dome, considering its formation due to a region of high atmospheric pressure that trapped hot air at the earth's surface; henceforth we employ the term PNW heat dome to refer to this specific event, acknowledging that heatwaves may in general be due to other mechanisms^{6,8}.

The PNW heat dome also had a pronounced effect on the 2021 fire season, with record high temperatures and atmospheric moisture deficits

producing extreme fire weather conditions over a large area for an extended period of time, enabling synchronous wildfire activity. These conditions were also associated with extreme fire behaviour including frequent episodes of night-time burning and large pyro-cumulonimbus (pyroCB) events initiated by the extreme heat generated by several of the large fires. One such massive pyroCB, initiated by the Lytton and Sparks Lake fires, generated over fifty thousand cloud-to-ground lightning strikes over an eight hour period starting on June 30th (data from the Canadian Lightning Detection Network⁹, starting further fires.

There is a well-established link between large-scale (ie. synoptic) atmospheric patterns — such as the large amplitude ridge that caused the heat dome — and surface fire weather conditions that contribute to fire spread. Specifically, synoptic-scale weather analyses have shown that ridge-like patterns in upper-air tropospheric flow are frequently associated with atmospheric blocking events and that such events promote fuel aridity and fire activity^{10–15}. Blocking ridges were identified as key drivers of the 6.7 Mha that burned in Canada in 1989, being one of Canada's most significant fire seasons¹⁶. Recently, in the spring and summer of 2023, blocking events occurred asynchronously in both the west and east of Canada, leading to well above seasonal temperatures and

¹Natural Resources Canada, Canadian Forest Service, Northern Forestry Centre, Edmonton, AB, Canada. ²Future Forest Ecosystems Centre (FFEC), BC Ministry of Forests, Kamloops, BC, Canada. ³Department of Renewable Resources, University of Alberta, Edmonton, AB, Canada. ⁴Management of Complex Systems, University of California, Merced, CA, USA. ⁵Natural Resource Science, Thompson Rivers University, 805 TRU Way, Kamloops, BC, Canada.

✉ e-mail: piyush.jain@nrcan-rncan.gc.ca

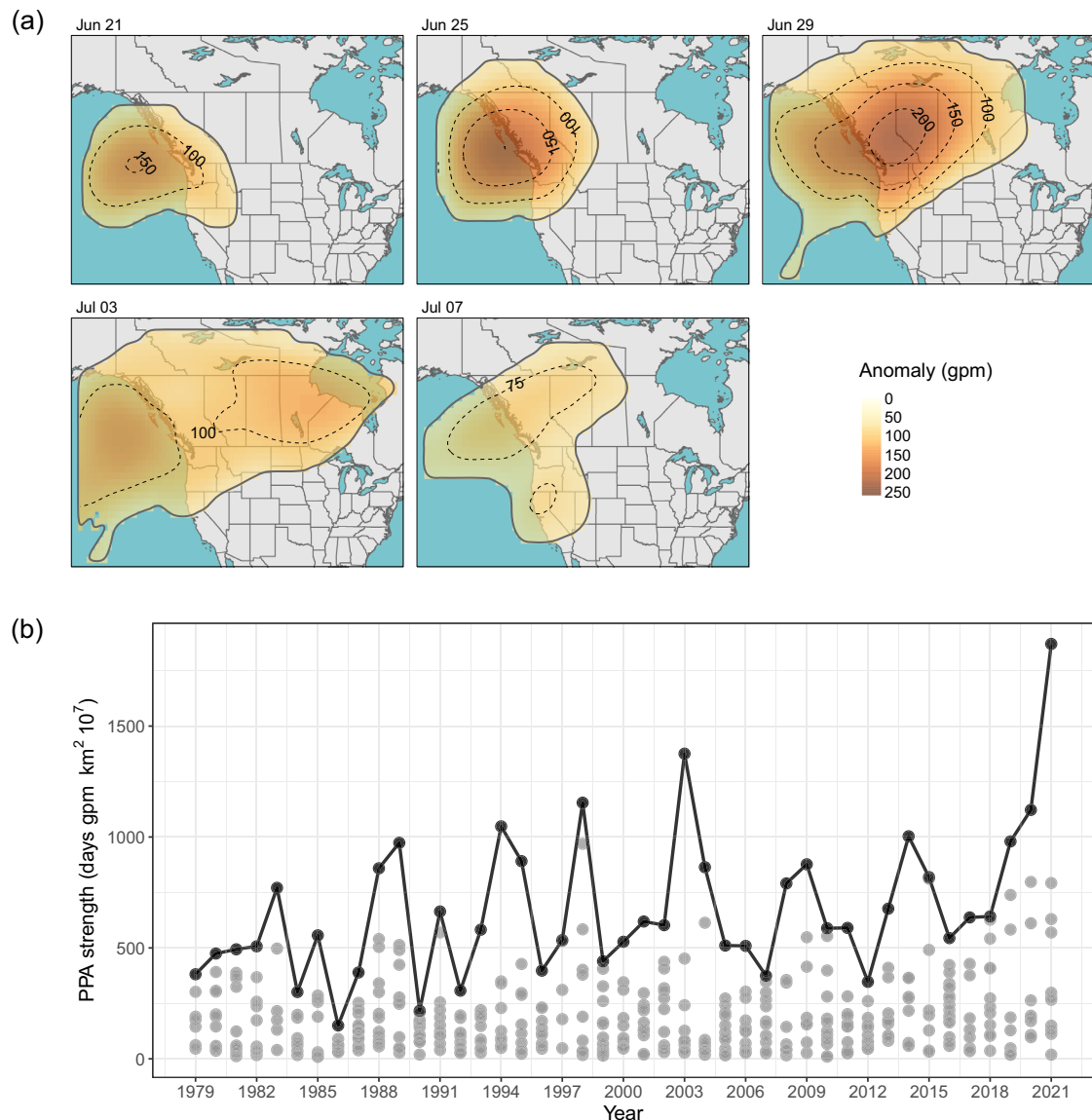


Fig. 1 | Evolution and strength of the 2021 PNW heat dome. The two largest persistent positive anomaly (PPA) events in North America for 2021 and a comparison of largest PPA events from 1979–2021. **a** The temporal and spatial evolution of the largest PPA event occurring in JJA, corresponding to the PNW heat dome.

500hPa geopotential height anomalies are in units of geopotential meters (gpm); **b** Time series of the PPA strength of the maximum PPA (black) and other PPA events (grey) that occurred during JJA of each year 1979–2021.

precipitation deficits, exacerbating the extraordinary fire season where approximately 15Mha burned in Canada in 2023¹⁷. developed a method for tracking these types of events in terms of so-called persistent positive anomalies (PPAs) in 500-hPa geopotential heights. They found that PPAs were strongly associated with wildfire ignitions, large fires, and area burned for western North America.

In this paper we examine the 2021 North American fire season through the lens of the PNW heat dome. To do this we apply the PPA tracking algorithm developed in ref. ¹⁷ to the 2021 event; this allows us to perform an event-level analysis in order to quantify the exceptional nature of the 2021 event in terms of other such events that occurred during the available historical period and examine its influence on fire weather extremes and observed fire activity. We partially attribute the event to climate change by comparing the observed event to that estimated after removing the background warming. We also discuss the considerable constraints placed on fire management and how this relates to the synchronous fire danger observed in 2021.

Results and discussion

Large-scale drivers and the 2021 heat dome

The 2021 Pacific Northwest heat dome along with other similar atmospheric blocking events can be identified by tracking persistent positive anomalies (PPAs) in the mid-tropospheric 500 hPa geopotential heights¹⁷. We identified a total of 11 PPA events that lasted at least 5 days that occurred between June and August 2021 in North America (Supplementary Table 1, see methods for details). The evolution of the largest of these events is shown in Fig. 1a corresponding to the PNW heat dome that started June 18th and ended July 14th (lasting 27 days). The PNW heat dome itself was the result of an extreme and persistent high-pressure ridge formed by high amplitude meridional, anticyclonic flow of the tropospheric jet stream which brought in warm air from lower latitudes, coincident with a stable stratification within the block which trapped heat at the surface¹⁸. The event itself was further amplified by moderate positive feedbacks between antecedent drought conditions and the heatwave¹⁹, as well as by an incursion of a trans-Pacific atmospheric river that brought excess sensible heat and moisture

into the region²⁰. The associated PPA event started in mid-June in the Pacific Northwest of the United States, strengthening and expanding in size during the last week of June (Fig. 1a). The maximum magnitude in 500hPa geopotential height anomalies occurred on June 25th. During the last few days of June and first few days of July the PPA further expanded encompassing regions in central and eastern Canada (ie. Manitoba and Ontario), reaching its maximum size on July 3rd and then subsequently receding and contracting before disappearing by mid-July.

The exceptional nature of the PNW heat dome is evident in Fig. 1b that shows the time series of the strength (defined as the area weighted event magnitude summed for all days of the event) for all PPA events identified in June, July or August (JJA) of each year for 1979–2021. In total we identified 450 PPA events in the study region for this time period during JJA (approximately 10.5 per year). The 2021 PNW heat dome had the largest strength occurring of these events, lasting 27 days, with a maximum area of 11.6×10^6 km² and a maximum 500hPa geopotential height anomaly of 241 m. The next strongest event in the time series was 36% weaker and occurred in July–August 2003. The PNW heat dome was also 2.9 times stronger than the average of annual maximum PPA from 1979–2020.

Extreme weather events such as the PNW heat dome are also increasingly being attributed to anthropogenic climate change⁷. Here we quantify the amplification of the heat dome event due to anthropogenic background warming by using the implicit relationship between warming and geopotential heights²¹. Figure 2 shows the difference in the attributes between the observed heat dome and the equivalent event after removing the historical linear trend in geopotential heights, equivalent to removing

the warming trend of the lower atmosphere (methods). We found that the PNW heat dome was 59% longer (27 days duration versus 17 days), 34% larger and had 6% higher maximum amplitude, comparing the observed event and the event after detrending. Overall the strength of the heat dome was 86% greater than the same event would have been without background warming.

Fire weather records and anomalies

The PNW heat dome led to extraordinary fire weather extremes over western North America. Table 1 provides a summary of the records broken in 2021 during the entire year and within the spatiotemporal extent of the heat dome for a number of fire weather metrics. Specifically, this event led to record breaking values of maximum daily temperature and Vapor Pressure Deficit (VPD) over large areas of western North America in 2021 as evident in data from the ERA5 reanalysis over the historical period from 1979–2021 (see Fig. 3a and b). Maximum daily temperature records broken during 2021 accounted for 14% of all grid cells over Canada and the United States, with 86% of those records occurring within spatiotemporal extent of the PNW heat dome. Similarly, the percentage of maximum daily VPD records broken during 2021 were 11.5% with 80% of these records occurring within the spatiotemporal extent of the PNW heat dome. Conversely, an output of the Canadian Fire Weather Index System (CFWIS), daily Canadian Fire Weather Index (FWI) showed relatively few records (3%) for 2021, only 14% of which occurred during the PNW heat dome (Fig. 3c). The fact that FWI did not exhibit a large number of records in 2021 despite the extreme high temperatures and low atmospheric humidity is likely due to the fact that surface wind speeds (one of the inputs to the FWI System) remained close to normal during the PNW heat dome as shown in Supplementary Fig. 1, which shows anomalies for the FWI input variables for 2021. In fact ref. ²², showed that during extreme fire weather events, the FWI can be particularly sensitive to wind speed. Similar results were seen for the Hot-Dry-Windy Index (HDWI) that combines VPD and wind speed (Supplementary note 1, Supplementary Fig. 2).

Nighttime fire weather conditions were also extreme in 2021: the percentage of mean nighttime temperature records broken during 2021 were 12%, 85% of which occurred during the heat dome (Fig. 3d) and the percentage of mean nighttime VPD records broken were 7.7%, 67% of which occurred during the PNW heat dome (Fig. 3e). To assess nighttime burning conditions from the CFWIS, we also considered nighttime mean values of the hourly Fine Fuel Moisture Code (FFMC), which use surface temperature, relative humidity, precipitation and wind speed. For nighttime FFMC, only 2.9% of records were broken in 2021, 31% of which occurred during the PNW heat dome (Fig. 3f). Similar to the FWI (and the HDWI) records, the difference is likely because larger wind speeds were not coincident with higher temperatures and lower humidity at night time.

We further considered anomalies in maximum daily temperature, VPD and FWI for three different scenarios: during and within the spatial extent of the PPA corresponding to the heat dome (PPA_{HD}), for all other PPAs (PPA_{small}) that occurred in the study area from April to September,

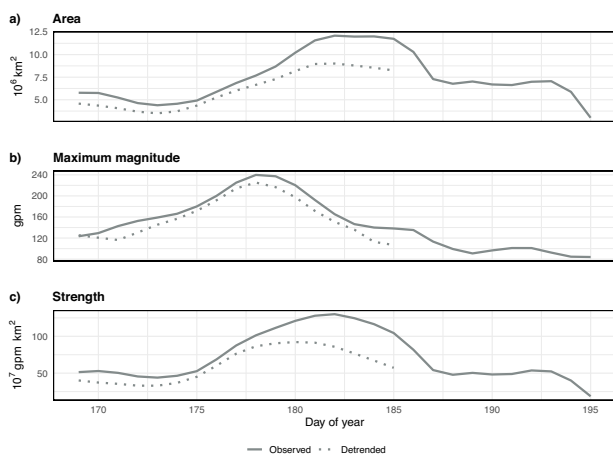


Fig. 2 | Temporal evolution of 2021 PNW heat dome attributes. Time-dependent attributes of the observed heat dome (solid line) and the equivalent event (dotted line) after detrending the 500 hPa heights (“counterfactual”); **a** spatial area of event; **b** the maximum magnitude of event; and **c** the strength (sum of magnitude and area of each grid cell identified as part of event).

Table 1 | Fire weather records broken in 2021 for period 1979–2021

Variable	Percent records broken in 2021	Rank of records broken in 2021	Percent of 2021 records occurring in PNW heat dome	Area records broken in 2021 (10 ⁶ km ²)	Rank of area records broken in 2021
Tmax	14.05	1	86.72	2.91	1
FWI	2.67	13	14.18	0.58	12
VPDmax	11.50	1	81.15	2.42	1
FFMC _{night} (mean)	2.90	14	30.64	0.66	12
T _{night} (mean)	11.86	1	85.63	2.54	1
VPD _{night} (mean)	7.72	1	67.17	1.72	1
HDW	10.21	1	80.25	2.10	1

Percent fire weather records broken in 2021, using reanalysis data from 1979–2021. The percentage of records broken represents the number of grid cells with a record breaking value in the study area; the corresponding spatial area is also given. 2021 had the highest percentage and spatial area for records broken in 2021 for Tmax, VPDmax, T_{night} (mean), VPD_{night} (mean) and HDW. See main text for description of individual variables.

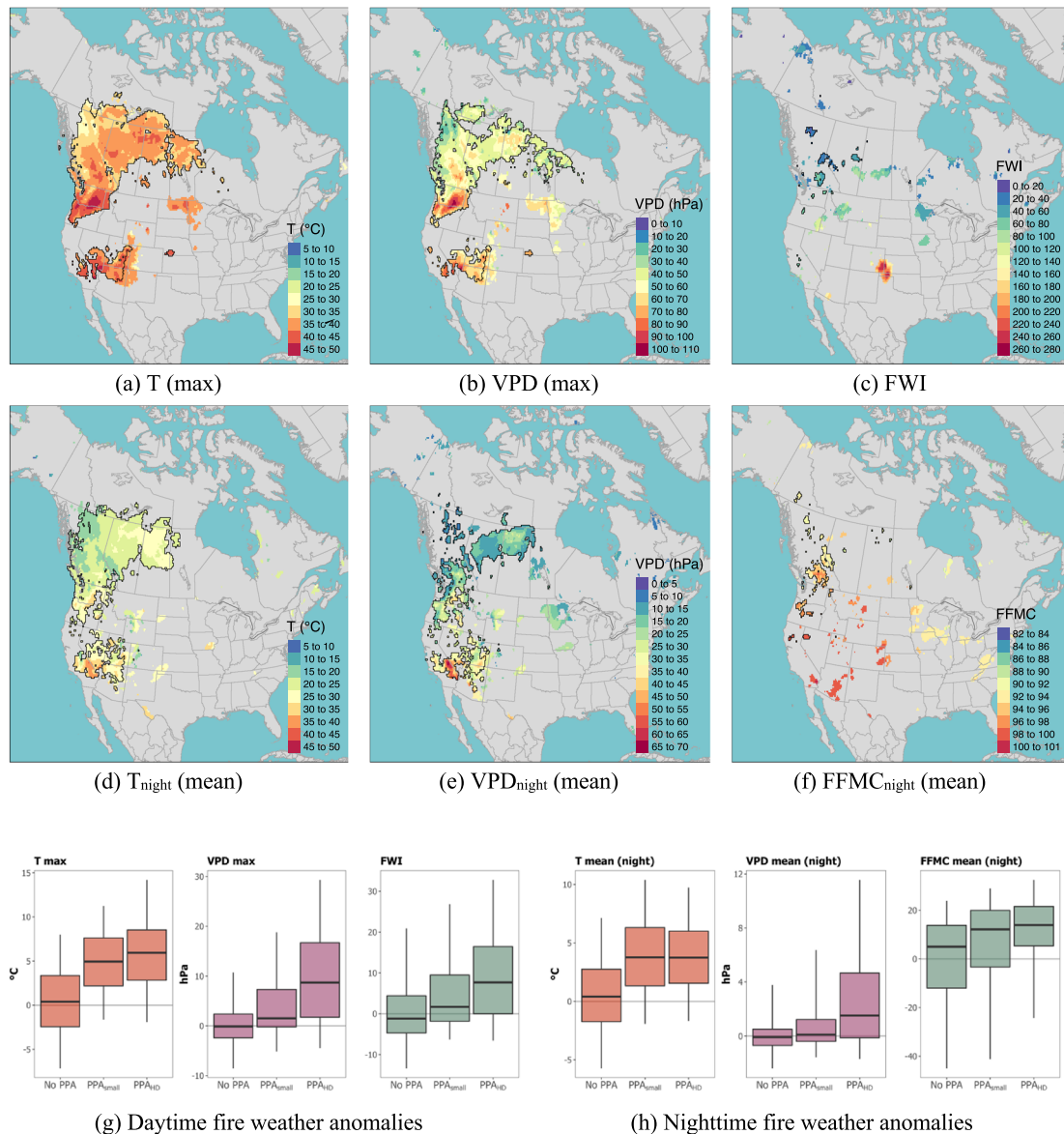


Fig. 3 | Fire weather records and anomalies during 2021. Record values that occurred in 2021 for several fire weather variables, and fire weather anomalies for 2021 relative to historical record 1979–2020: 2021 records for **a** maximum daily temperature; **b** Maximum daily VPD; **c** FWI; **d** Maximum mean nighttime temperature; **e** Maximum mean nighttime VPD; **f** Maximum mean nighttime FFMFC. Records broken within the heat dome event are further outlined in black; **g** Daytime

fire weather anomalies when no PPA occurred, for all smaller PPA events (PPA_{small}) and the PPA corresponding to the heat dome (PPA_{HD}); **h** night-time fire weather anomalies as per panel **g**. Nighttime here is defined as 10 pm–6 am local standard time. (For each anomaly, center line is the median, interquartile range, and upper and lower values are 95th and 5th quantiles respectively).

and in the absence of any PPA. The largest anomalies in daytime burning conditions occurred within the heat dome event with positive anomalies also occurring for other PPA events (Fig. 3g). Night-time fire weather anomalies were also estimated for temperature, VPD and Fine Fuel Moisture Content (FFMFC); here night-time values were calculated as the mean values of the respective variable between 10 pm and 6am (local standard time). Similar to the daytime values we also found the largest anomalies in night-time burning conditions occurred within the heat dome event with positive anomalies also occurring during other PPA events (Fig. 3h).

These results highlight the role that PPA events play in causing above-normal surface temperatures while diverting atmospheric moisture and precipitation through anticyclonic blocking. In general, it should be noted that the strength of the relationship between upper air large-scale atmospheric patterns and surface fire weather conditions vary by geographic location across North America^{10,17} showed that some of the strongest

correlations between PPA days and warm dry surface conditions occur in the PNW. This is consistent with the presence of the “Pacific High”, a semi-permanent atmospheric ridge that exists over Western North America^{10,12,15}.

Fire activity

Driven by weather extremes including the PNW heat dome event, 2021 was a well-above average year for wildland fire in North America. Satellite-based estimates of area burned based on the Moderate Resolution Imaging Spectroradiometer (MODIS) area burned product (MCD64A1) indicate a combined area of 7.51 Mha burned in the United States and Canada in 2021, which is the highest annual value in the available data for that dataset (2002–2021; Fig. 4a). Preliminary agency records from the National Inter-agency Fire Centre (NIFC) for the United States and quality-controlled data from the National Burned Area Composite (NBAC) for Canada indicate a combined area of 7.46 Mha burned over the same region in 2021; this value is the 5th highest in the agency data record (1986–2021; Supplementary

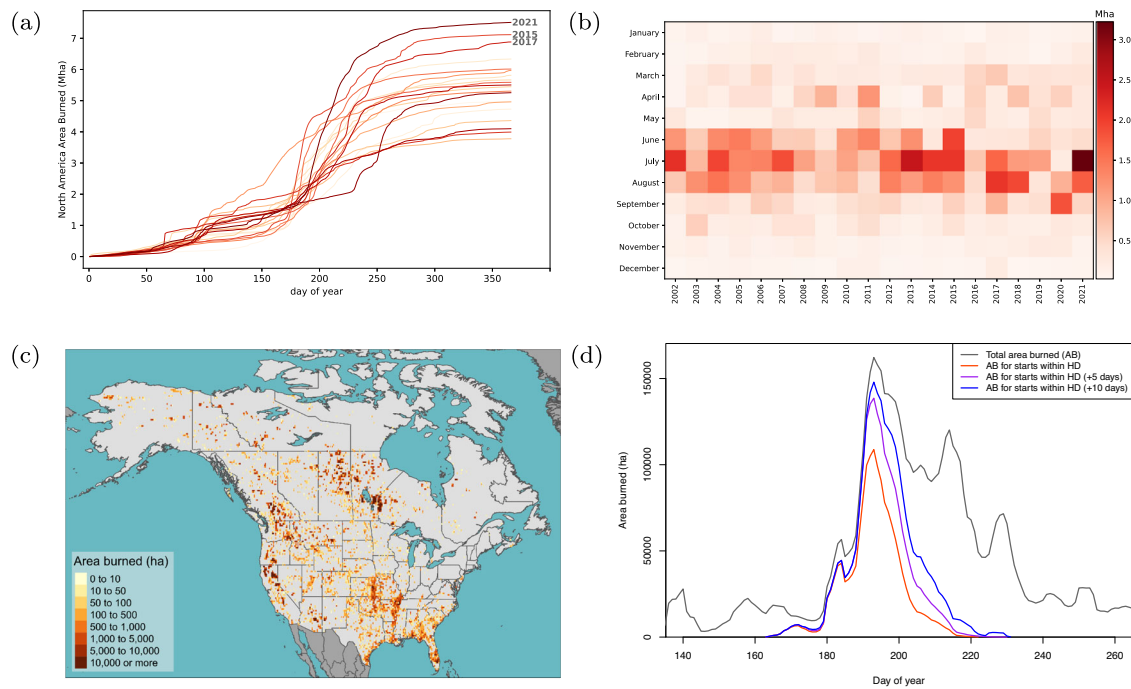


Fig. 4 | Temporal and spatial characteristics of area burned in North America for 2021. **a** cumulative area burned (millions of hectares, Mha) from the MODIS area burned product (MCD64A1) for North America for each year between 2001–2021; **b** MCD64A1 estimates of area burned for the contiguous United States and for Canada; **c** the spatial distribution of burned area in North America using MCD64A1, regridded at 0.25 deg resolution; **d** time series of the total area burned in North America (grey points) with 5-day moving average shown by the grey shaded area; the

red shaded area represents the area burned for any continuous burn periods that started within the spatiotemporal extent of the PNW heat dome (after applying a 5-day moving average); the purple and blue curves represent the area burned for any continuous burn periods that started within the spatiotemporal extent of the PNW heat dome or up to 5 or 10 days later (after applying a 5-day moving average), respectively.

Fig. 3) and the 3rd highest for the same period as the MODIS burned area record. The differences between these two estimates reflects the uncertainty that exists in both the MODIS and NIFC datasets (see Supplementary Fig. 4). In spite of this uncertainty in the area burned estimates, in July 2021 alone, over 3.2 Mha burned according to the MODIS area burned product, representing the highest burned area in any single month from 2002–2021 (Fig. 4b).

Using the MODIS area burned estimates (see Supplementary Table 2) the greatest area burned during 2021 occurred in Manitoba (1.0 Mha; 0.96% of land area), California (0.9 Mha, 2.2%), Saskatchewan (0.8 Mha, 0.74%), British Columbia (0.7 Mha, 0.48%) and Ontario (0.7 Mha, 0.40%). For these regions, the majority of area burned occurred in July, with the exception of California where the majority of area burned occurred in August. Manitoba and Ontario both had a record area burned in 2021 (2002–2021). Significant July burning also occurred in Oregon and Washington. Overall, July was the month with the most area burned (3.2 Mha) with extensive burning over much of the continent (see Fig. 4, panels c and d). Further north, Alaska and North West Territories experienced below average burning but followed the usual seasonal pattern with greatest area burned occurring in July and August.

To examine the influence the PNW heat dome had on fire activity, we further used the MODIS area burned product (regridded to 0.25 degree resolution) to estimate the area burned during the PNW heat dome as follows: for each grid cell we identified all continuous burn periods that started within the spatiotemporal extent of the PPA. Here a continuous burn period is any consecutive sequence of days where the area burned is greater than zero. We then summed the area burned for all such sequences over all grid cells and divided by the total area burned (for North America) to determine the percentage area burned under the PPA (see Fig. 4d). We found 20.6% of the total area burned was associated with the PNW heat dome PPA with a further 15% associated with the other PPA events. Further accounting for daily burned area up to 5 days and 10 days after the PNW

heat dome increased the burned area associated with the PNW heat dome to 28% and 34% of annual totals, respectively.

Constraints on Fire management resources

The substantial area burned and the extreme fire behaviour, much of which can be attributed to multiple synchronous fire events that occurred during and after the PNW heat dome, challenged fire management agencies across North America. In Canada, member agencies (consisting of provincial and territorial fire management agencies and Parks Canada) report preparedness levels to the Canadian Interagency Forest Fire Centre (CIFFC); In the United States, 10 separate Geographic Area Coordination Centers (GACCs) report preparedness levels to the National Interagency Fire Center (NIFC). There are five preparedness levels (1 to 5) determined by a combination of situational awareness elements²³. The national agencies (CIFFC and NIFC) assimilate preparedness levels from member agencies to determine a National Preparedness Level (NPL) in each country, representing the level of national fire hazard and resource demand. Higher preparedness levels represent increased fire activity and greater need for resource sharing between agencies; specifically, levels 4 and 5 require *high* and *extreme* resource demand respectively. Widespread synchronous fire activity has been found to be highly correlated with high resource demand days with $NPL \geq 4$ in the western United States^{24,25} also explored the relationship between fire management decision scales and scales of fire weather, highlighting the role of synoptic scale weather features such as the PPA events discussed here.

NPL values during 2021 were well above average in both Canada and the US as shown in Fig. 5a. In fact, 2021 had a record number of days at both $NPL = 4$ or 5 ($NPL = 4+$) for both countries as shown in Fig. 5b, when compared with all other years with reported data (2003–2021). In particular the NIFC and the CIFFC respectively reported 69 and 50 days at $NPL = 5$, most of which occurred during July for Canada and July and August for the US. This sustained period of the highest preparedness level is indicative of

the extreme demand for fire management resources in multiple jurisdictions in both countries. Of particular interest, the number of days with either NPL = 4 or 5 occurring simultaneously in both countries was 63, whereas the number of days with NPL = 5 occurring simultaneously was 47. During this period with NPL = 5 occurring simultaneously in both Canada and the US resource sharing between the two countries was severely constrained, further hindering fire suppression efforts²⁶.

Following²⁴, we further investigated the relationship between synchronous fire danger and the number of days with NPL = 4+ for Canada and the US, highlighting the role of the PNW heat dome in promoting synchronous fire danger over a broad area. The correlation between the annual number of days with NPL = 4+ and synchronous fire danger for Canada (defined as number of days with FWI > FWI₉₅ exceeding 10% of the forested suppression zone; see methods) was 0.8, whereas for synchronous fire danger in the US (days with FWI > FWI₉₀ and exceeding 24% of forested suppression zone; see methods) was 0.79. For 2021, we identified 39 days of synchronous fire danger in Canada and 46 in the US. The robust correlation between NPL = 4+ and synchronous fire danger is also apparent for 2021 in Fig. 5a and b for Canada and the US respectively, where the NPL for each country covaries with the spatial extent of synchronous fire danger in forested areas with historically high levels of fire suppression. In particular, the PNW heat dome represented a period of elevated synchronous fire danger during which the NPL was increased from 2 to 5 in Canada and 3 to 5 in the US.

Smoke and Evacuations

Smoke from wildfires can severely impact air quality with important implications for public health; a study of Canadian health outcomes attributed

long-term wildfire smoke exposure to 570–2500 premature mortalities per year²⁷. The widespread and synchronous burning that occurred in North America during 2021 also led to frequent episodes with high levels of wildfire smoke, dispersed over broad regions. This was particularly evident in July where an estimated 20–68 million people in North America were exposed to high levels of particulate matter (see methods for details). One of the most profound impacts of the 2021 fire season was the large number of people displaced by the threat of fire in their communities. Data from the Canadian wildfire evacuations database²⁸ showed 217 evacuation orders were issued in 2021 in Canada due to imminent danger from wildfires, the highest number in the available record (1980–2021). The overwhelming majority of these events (181) occurred in British Columbia with 93 evacuations issued in July alone with a further 65 issued in August. In total more than 50 thousand people were evacuated, which was the third on record (1980–2021) behind 2003 and 2016. In 2016 more than 100 thousand people were evacuated due largely to the evacuation of the entire population of Fort McMurray (Alberta) during the Horse River fire that occurred in May of that year.

Conclusion

The 2021 North American fire season was extraordinary by several measures. The greatest area burned in a single month on recent record (2003–2021) occurred in July with 3.2 Mha burned. Record-breaking hot and dry weather conditions occurred considering both maximums in daily temperature and minimums in vapor pressure deficit values. There was widespread and synchronous wildfires that strained fire management with national preparedness levels set at the highest level of 5 for 69 days in the US and 50 days in Canada, both being record numbers in the period 2003–2021. There was also widespread and high levels of wildfire smoke that impacted

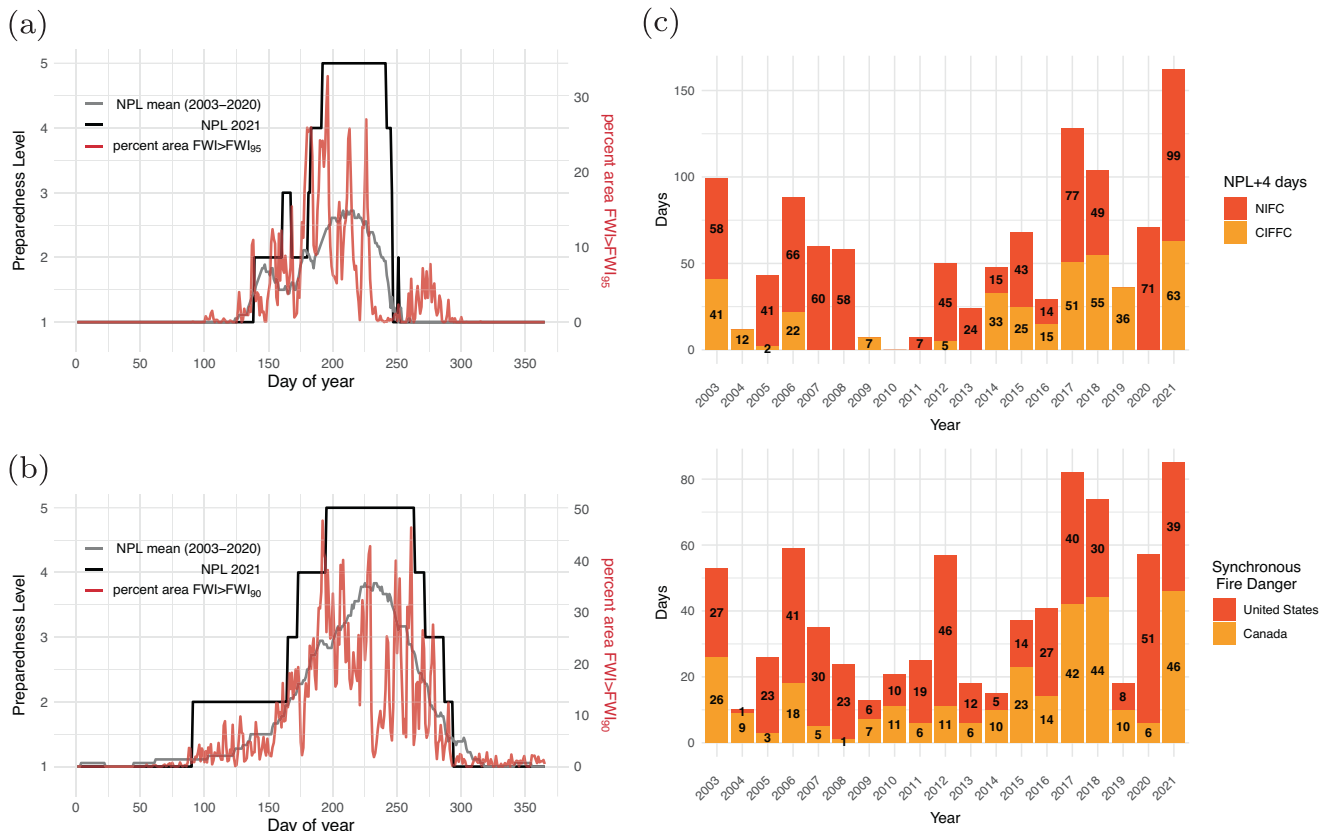


Fig. 5 | Preparedness levels and synchronous fire danger. a Preparedness levels (PLs) for day of year for the Canadian Interagency Forest Fire Centre (CIFFC) for 2021 compared with mean values for 2003–2020 and percent of forested full suppression zone in Canada with FWI exceeding 95th percentile; b PLs for day of year for the National Interagency Fire Center (NIFC) for 2021 compared with

mean values for 2003–2020 and percent of western US forests with FWI exceeding 90th percentile; c top: Annual number of PL = + 4 days for CIFFC and NIFC between 2003 and 2021; bottom: Annual number of days with synchronous fire danger for the western US forests and the forested full suppression zone of Canada.

an estimated 20–68 million people in July estimated using two different measures and 217 evacuation orders in Canada alone.

The severity of the 2021 fire season was unequivocally intensified by the presence of the heat dome that formed over the Pacific Northwest at the end of June and lasted well into July, and the various ways in which it affected surface weather and fire behaviour. Twenty one percent of the total area burned in 2021 in North America was due to fires that started during and within the heat dome, this number rising to 34% of the total for fires starting within 10 days of the event. Apart from the effects of wildfires, this exceptional heat-wave event caused record-breaking temperatures with 49.6 °C recorded at Lytton, British Columbia, and was attributed to 619 heat-related deaths in British Columbia over a period of a single week with further significant fatalities in Washington and Oregon.

We were able to quantify the exceptional nature of the heat dome using a method developed by¹⁷ and we found it was 36% stronger and had 38% larger maximum area than the next largest event of this type that occurred in August 2003 using data from 1979–2020.

Similar to other extreme weather events, one should consider the 2021 Pacific Northwest heat dome in the context of anthropogenic climate change. Globally, there are clear trends in increasing extreme fire weather and decreasing fuel moisture^{29,30}. The conjecture that the rapid warming observed in the Arctic also points to evidence for a wavier polar jet stream, which in turn, may lead to the more frequent occurrence of extreme weather patterns in the mid-latitudes has been well documented (eg. ^{31–33}). However, more recent work suggests the case for this may be overstated^{34,35}. Here, using a simple attribution method that does not invoke amplification of Rossby waves, the 2021 heat dome was estimated to be 59% longer, 34% larger and had 6% higher amplitude than the same event would have been without background warming.

This is consistent with results from¹⁷ who found that while the size and magnitude of heat-waves is increasing in western North America, the frequency of these events is not changing significantly. In other words, continued thermodynamic changes due to anthropogenic warming will likely make these events larger and more intense in the future. When such events are associated with widespread synchronous fire activity, this may challenge future fire management efforts beyond their available resources.

Methods

Study area

The study area used for this analysis included Canada, Alaska and the continental United States (CONUS). This large study area contains several pyro-biomes that are dominated by either temperate or Boreal forest systems. Many North American ecosystems with burnable biomass experience frequent wildland fire, albeit with substantial interannual variability depending on the interaction of possible ignitions with fuel moisture, the presence of fire conducive weather and fire management actions. In Canada, where the majority of forested area is Boreal forest, 2.1 Mha burns annually on average; In the United States, the average area burned since 2000 has been 2.8 Mha, although this figure is increasing, predominantly driven by increased fire activity in the western US in recent years^{36,37}.

PPA identification

To identify atmospheric blocking events, such as the one that resulted in the extreme June–July heatwave of 2021 in western Canada and the Pacific Northwest region of the United States, we implemented an algorithm based on tracking persistent positive anomalies (PPAs) of the geopotential height field at 500 hPa (Z500), following ref. ¹⁷. Geopotential height values were obtained from the ERA5 global climate reanalysis³⁸, regridded to 1 degree horizontal resolution and averaged to give daily mean values. We then calculated the 5-day running mean latitude-weighted Z500 anomalies (Z') following³⁹:

$$Z' = \frac{(\sin 45^\circ)}{(\sin \varphi)} (Z - \underline{Z}) \quad (1)$$

where φ is the latitude of the grid cell, Z is the 5-day running mean of Z500 and \underline{Z} is the climatological value of Z500 for a given day of year (for the period 1979–2021). We implemented a feature tracking algorithm using three criteria to identify potential heatwave events. The first criterion isolates potential PPA grid cells from the background anomalies as any contiguous regions with magnitude $> M$, where M is defined as one standard deviation of the daily Z' values using a 4-week moving window following⁴¹. A second criterion is then applied where only those grid cells that persist for at least five days are retained. Finally, for each identified cluster only days where the contiguous PPA area is greater than $\sim 80,000$ km² within the study domain are retained (equivalent to 16 grid cells at 45°N). Using this algorithm one can track the location of the geometric centroid, the duration, the spatial extent (area) and the magnitude (500hPa geopotential height anomaly) of each grid cell corresponding to the PPA event. We defined daily PPA strength as the area weighted sum of the event magnitudes of all grid cells corresponding to the identified event on a given day. The total strength of a given PPA event was then defined as the daily strength summed over the duration that event. This PPA-based approach highlights the anomalous two-dimensional area of atmospheric blocking, and has been widely used^{39–43}. Here we use a modified algorithm with daily varying magnitude thresholds as it is better suited for the identification of boreal summer PPA events¹⁷. Using this algorithm, we identified PPA events over the domain covering 35°–75°N and 60°–149°W within which the June 2021 PNW heat dome exerted its influence. Moreover, we identify the PPA events in two time periods: (i) from June–August (JJA PPA), the period that contains the duration of the heat dome and (ii) May–September (May–Sep PPA) to characterise fire weather anomalies during the extended fire season.

Event attribution

Observed positive trends in 500-hPa have previously been linked to anthropogenic forcings and the thermodynamic expansion and warming of the lower atmosphere²¹. To determine the role of anthropogenic warming, we detrend the 500 hPa geopotential heights by removing the linear trend (between 1979–2020) estimated by the Theil–Sen slope estimator. We then recalculate the PPA characteristics on the detrended geopotential heights and identify the equivalent detrended event (that would be equivalent to a “counterfactual” in a formal attribution study) as the event that coincided in space and time with the observed event. As noted in¹⁷, this results in quantitatively similar results when detrending the difference (thickness) between the 500 hPa and 1000 hPa geopotential heights. Moreover, given nominal changes in 1000hPa heights, changes in 500hPa heights should be a function of changes in mean temperature integrated between 1000–500hPa per the hypsometric equation. This form of attribution analysis, only using observational data, has previously been outlined by ref. ⁴⁴ as an alternative to standard methods that use climate models to model both observed and counterfactual event distributions. However, because of the anomalously large magnitude of the 2021 PNW PPA we were not able to estimate the return period of the event nor therefore calculate the increased likelihood of the event due to climate change as per the usual notion of formal attribution⁴⁵.

Area burned data

Historically, the best estimates of burned area in Canada and the United States due to wildland fire are provided respectively by the National Burned Area Composite (NBAC⁴⁶) and the Monitoring Trends in Burn Severity (MTBS⁴⁷). However, as neither of these data products included data for 2021 wildfires at the time of writing we used alternative estimates of burned area for this study. The MODIS burned area product Collection 6 (MCD64A1 v006), which provides an estimate of daily burned area, was regridded to 0.25 degree horizontal resolution to match the spatial resolution of the gridded weather data. Alternative estimates of area burned were also provided by the Canadian Interagency Forest Fire Centre (CIFFC) and the National Interagency Fire Centre (NIFC).

Surface Fire weather conditions

We assessed daytime fire weather using maximum daily temperature (T_{\max}), maximum daily Vapor Pressure Deficit (VPD_{\max}) and daily values of the Fire Weather Index (FWI), the latter being part of the Canadian Fire Weather Index System⁴⁸. The FWI represents potential fire intensity by integrating temperature, precipitation, wind speed and relative humidity at the surface⁴⁹. VPD, which represents the difference between the actual amount of moisture in the atmosphere to the potential moisture in a saturated atmosphere, is a useful metric for estimating fuel aridity and has strong relationships with fire ignition and spread^{50,51}. These fire weather metrics were calculated using data from the ERA5 reanalysis, available hourly at 0.25 degree horizontal resolution⁵². Specifically, VPD was calculated using 2 m temperature and 2 m dewpoint temperature using a standard approximation⁵³. FWI values were calculated according to the overwintering procedure which adjusted startup spring drought conditions using values from the previous autumn in areas with snow cover over winter⁵⁴. For night-time burning conditions (defined as mean values during 10pm–6am local time), we also considered the Fine Fuel Moisture Code (FFMC), another output of the FWI System. FFMC represents fuel moisture of fine litter on the forest floor and can be calculated each hour using hourly weather inputs⁵⁵, although in general corrections may be necessary at night due to decoupling of surface temperatures from 2 m observations during stable nocturnal stratification under a sparse canopy⁵⁶. For night-time burning conditions we also considered mean night-time temperature (T_{night}) and mean night-time VPD (VPD_{night}). FWI and FFMC were calculated using the CFFDRS R Package⁵⁷.

National Preparedness Levels and synchronous fire danger

Daily national preparedness levels (NPL) are determined for Canada by the Canadian Interagency Forest Fire Centre (CIFFC) and for the United States by the National Interagency Fire Center (NIFC). We calculated the mean value by day of year for each country using available data the period 2002–2020 where the two datasets overlap. We represented days of elevated resource demand (or limited resource availability) when $PL = +4$ (ie. 4 or 5). Following ref. ²⁴, synchronous fire danger was defined individually for each country as any day that the FWI values exceeded both a given threshold and a minimum area corresponding to a zone of enhanced fire suppression (EFS). For Canada, the EFS zone was determined by the full suppression zone⁵⁸ masked by forested area. For the US, the EFS zone used was the same as in²⁴, that is, the forested region of the contiguous US west of 103°W. The mask for forested area was constructed from the (MEaSURES) Vegetation Continuous Fields (VCF) Version 1 data product (VCF5KYR⁵⁹) as follows: percent tree cover from each year from 2001 to 2016 was composited into a single layer by taking the maximum value across years and then only including pixels with at least 2.5% tree cover. The resulting masked EFS region for Canada had an area of 4137683 km², whereas the masked EFS region for the US had an area of 1951440 km² (see Supplementary Fig. 5). Similar to the approach taken in ref. ²⁴, several country specific FWI and area thresholds were tested and those threshold values were chosen that gave the maximum Spearman correlation (ρ) between the annual number of days with synchronous fire danger and the annual number of days with $PL = +4$. For Canada, this corresponded to a threshold given by the 95th percentile of FWI (FWI_{95}) at each grid cell, and an area threshold of 10% ($\rho = 0.80$). For the US, this corresponded to a threshold given by the 90th percentile of FWI (FWI_{90}) at each grid cell and an area threshold of 24% ($\rho = 0.79$).

Smoke impacts

Air quality impacts from wildfire smoke are usually quantified in terms of ground level particulate matter (PM). Of particular concern is $PM_{2.5}$ which can negatively affect cardiopulmonary function. Because accurate determination of $PM_{2.5}$ requires direct ground monitoring, there will in general be incomplete monitoring of exposure during large smoke events. For this reason, satellite-derived Aerosol Optical Depth (AOD), a column integrated quantity, is often used as a proxy for $PM_{2.5}$ in epidemiological studies⁶⁰.

We downloaded monthly composites of Aerosol Optical Depth (AOD) derived from MODIS AQUA at 550 nm as per⁶¹. This data at 0.1 degree spatial resolution was resampled at 0.25 degrees and aggregated over the study area. For the monthly data used here we considered a threshold for prolonged smoke exposure risk corresponding to the 95th percentile of mean monthly AOD values using the available time series (July 2002–Sept 2021), which gave a value of $AOD_{th} = 0.34$. This compares with other estimates of risk thresholds, which use a daily mean AOD of 0.53 for vulnerable populations and 0.85 for the general population⁶². Here we further calculated two metrics for smoke exposure as (i) the land area with $AOD > AOD_{th}$; and (ii) the population exposed to $AOD > AOD_{th}$.

To calculate population exposure, we used gridded population density data (GPWv4; Center for International Earth Science Information Network CIESIN⁶³), which was available at 5 year intervals from 2000–2020 (5 layers) at 0.25 degree resolution. We estimated annual population density by linear interpolating these values and by setting the 2021 population density to that of 2020. Land and population exposure were then estimated by the sum of land area or population masked by the AOD risk threshold.

Because of the uncertainty in ground-level smoke exposure estimates from AOD, in part due to the regional variability in the strength of the relationship⁶⁰, we also considered model estimates of $PM_{2.5}$ from the Modern-Era Retrospective analysis for Research and Applications, Version 2 (MERRA-2⁶⁴). Similar to AOD, we used a threshold for smoke exposure based on the 95th percentile of mean monthly $PM_{2.5}$ values, which gave a value of $PM_{2.5th} = 27.0 \mu\text{g}/\text{m}^3$. This value is consistent with the National Ambient Air Quality Standards (NAAQS, <https://www.epa.gov/pm-pollution/national-ambient-air-quality-standards-naaqs-pm>) for $PM_{2.5}$ which is annual mean levels of $12 \mu\text{g}/\text{m}^3$ or $35 \mu\text{g}/\text{m}^3$ daily mean levels. Similar to the case of AOD outlined above, we calculated smoke exposure as (i) the land area with $PM_{2.5} > PM_{2.5th}$; and (ii) the population exposed to $PM_{2.5} > PM_{2.5th}$.

We used monthly values of AOD derived from MODIS to determine prolonged wildfire smoke exposure in terms of both land area and population (see Supplementary Fig. 6, panels a and b). Based on this data we found that compared with the period for which data was available (July 2002–September 2021) that July 2021 was the month with the greatest land area exposure ($\sim 7.7 \times 10^6 \text{ km}^2$) and population exposure (~ 68 million people) due to wildfire smoke. Since AOD is a column integrated quantity and does not necessarily reflect ground level smoke levels we also consider modelled monthly estimates of surface $PM_{2.5}$ from the MERRA-2 reanalysis (see Supplementary Fig. 6). Using MERRA-2 we found that July 2021 had the 2nd greatest land area exposure ($\sim 3.3 \times 10^6 \text{ km}^2$) and the 14th greatest population exposure (~ 20 million people). For the MERRA-2 data August 2021 was the month of greatest monthly; exposure to wildfire smoke covered an area of $\sim 3.3 \times 10^6 \text{ km}^2$, corresponding to population exposure of ~ 48 million people. This was the 2nd highest monthly area exposure value and 5th highest monthly population exposure value for the MERRA-2 data (using data from January 2000–December 2021).

Data availability

PPA data generated during this study are available at the Centre for Open Science OSF data repository (<https://doi.org/10.17605/OSF.IO/VU7N9>). Gridded observations of upper level and surface weather from the ERA5 reanalysis was downloaded from the European Centre for Medium-Range Weather Forecasts (ECMWF), Copernicus Climate Change Service (C3S) at Climate Data Store (CDS; <https://cds.climate.copernicus.eu/>). The MODIS burned area product Collection 6 (MCD64A1 v006) was downloaded from Google Earth Engine (<https://doi.org/10.5067/MODIS/MCD64A1.006>). Agency estimates of area burned were downloaded from <https://www.ciffc.ca/> for Canada and <https://www.nifc.gov/> for the United States. National preparedness level data for the United States were downloaded from <https://www.nifc.gov/sites/default/files/2020-09/PreparednessLevels.xlsx> and for Canada was obtained by a request to the CIFFC. Percent tree cover was from the (MEaSURES) Vegetation Continuous Fields product (VCF5KYR, <https://lpdaac.usgs.gov/products/vcf5kyrv001/>). Aerosol Optical Depth data was

downloaded from the MODIS MYD04 product (https://doi.org/10.5067/MODIS/MYD04_L2.006). Monthly means of PM_{2.5} data was downloaded from the MERRA-2 reanalysis product (<https://doi.org/10.5067/FY616726UXSR>). Data from the Canadian Wildland Fire Evacuation Database was obtained by request to the Canadian Forest Service.

Received: 11 October 2022; Accepted: 26 March 2024;

Published online: 22 April 2024

References

- White, R. H. et al. The unprecedented Pacific Northwest heatwave of June 2021. *Nat. Commun.* **14**, 727 (2023).
- BCCO report, Extreme Heat and Human Mortality: A Review of Heat-Related Deaths in B.C. in Summer 2021, British Columbia Coroners Office https://www2.gov.bc.ca/assets/gov/birth-adoption-death-marriage-and-divorce/deaths/coroners-service/death-review-panel/extreme_heat_death_review_panel_report.pdf, (accessed 2 September 2022).
- Multnomah County, (2021). <https://www.multco.us/multnomah-county/news/county-working-preliminary-report-june-2021-heat-wave-deaths-focusing-housing> (Accessed 11 September 2022)
- Washington State Department of Health, 2021. <https://doh.wa.gov/emergencies/be-prepared-be-safe/severe-weather-and-natural-disasters/hot-weather-safety/heat-wave-2021> (Accessed 11 September 2022).
- McKinnon, K. A. & Simpson, I. R. How unexpected was the 2021 Pacific Northwest heatwave? *Geophys. Res. Lett.* **49**, e2022GL100380 (2022).
- Thompson, V. et al. The 2021 western North America heat wave among the most extreme events ever recorded globally. *Sci. Adv.* **8**, eabm6860 (2022).
- Philip, S. Y. et al. Rapid attribution analysis of the extraordinary heatwave on the Pacific Coast of the US and Canada June 2021. *Earth Syst. Dynam.* **13**, 1689–1713 (2022)
- Wehrli, K. et al. The ExtremeX global climate model experiment: investigating thermodynamic and dynamic processes contributing to weather and climate extremes. *Earth Syst. Dyn.* **13**, 1167–1196 (2022).
- Kochtubajda, B. & Burrows, W. R. Cloud-to-Ground Lightning in Canada: 20 Years of CLDN Data. *Atmos. Ocean* **58**, 316–332 (2020).
- Schroeder, M. J. Critical fire weather patterns in the conterminous United States. Office of Meteorological Operations. Silver Spring, Maryland, USA (1969)
- Flannigan, M. D. & Harrington, J. B. A study of the relation of meteorological variables to monthly provincial area burned by wildfires in Canada (1953–80). *J. Appl. Meteor.* **27**, 441–452 (1988).
- Skinner, W. R. et al. A 500 hPa synoptic wildland fire climatology for large Canadian forest fires, 1959–1996. *Theor. Appl. Climatol.* **71**, 157–169 (2002).
- Gedalof, Z. E., Peterson, D. L. & Mantua, N. J. Atmospheric, climatic, and ecological controls on extreme wildfire years in the northwestern United States. *Ecol. Appl.* **15**, 154–174 (2005).
- Zhong, S. et al. Synoptic weather patterns for large wildfires in the northwestern United States—a climatological analysis using three classification methods. *Theor. Appl. Climatol.* **141**, 1057–1073 (2020).
- Jain, P. & Flannigan, M. The relationship between the polar jet stream and extreme wildfire events in North America. *J. Clim.* **34**, 6247–6265 (2021).
- Hirsch, K. G. & Flannigan, M. D., November. Meteorological and fire behavior characteristics of the 1989 fire season in Manitoba, Canada. In Proceedings of International Conference on Forest Fire Research, Nov (pp. 19–22) (1990).
- Sharma, A. R., Jain, P., Abatzoglou, J. T. & Flannigan, M. Persistent positive anomalies in geopotential heights promote wildfires in western North America. *J. Clim.* **35**, 2867–2884 (2022).
- Neal, E., Huang, C. S. & Nakamura, N. The 2021 Pacific Northwest heat wave and associated blocking: Meteorology and the role of an upstream cyclone as a diabatic source of wave activity. *Geophys. Res. Lett.* **49**, e2021GL097699 (2022).
- Osman, M., Zaitchik, B. F. & Winstead, N. S. Cascading drought-heat dynamics during the 2021 Southwest United States Heatwave. *Geophys. Res. Lett.* **49**, e2022GL099265 (2022).
- Mo, R., Lin, H. & Vitart, F. An anomalous warm-season trans-Pacific atmospheric river linked to the 2021 western North America heatwave. *Commun. Earth Environ.* **3**, 1–12 (2022).
- Christidis, N. & Stott, P. A. Changes in the geopotential height at 500 hPa under the influence of external climatic forcings. *Geophys. Res. Lett.* **42**, 10–798 (2015).
- Dowdy, A. J., Mills, G. A., Finkle, K. & de Groot, W. Index sensitivity analysis applied to the Canadian forest fire weather index and the McArthur forest fire danger index. *Meteorol. Appl.* **17**, 298–312 (2010).
- Tymstra, C., Stocks, B. J., Cai, X. & Flannigan, M. D. Wildfire management in Canada: Review, challenges and opportunities. *Prog. Disaster Sci.* **5**, 100045 (2020).
- Abatzoglou, J. T., Juang, C. S., Williams, A. P., Kolden, C. A. & Westerling, A. L. Increasing synchronous fire danger in forests of the western United States. *Geophys. Res. Lett.* **48**, e2020GL091377 (2021).
- Taylor, S. W. Atmospheric cascades shape wildfire activity and fire management decision spaces across scales— A conceptual framework for fire prediction. *Front. Environ. Sci.* **8**, 527278 (2020).
- Bloem, S., Cullen, A. C., Mearns, L. O. & Abatzoglou, J. T. The role of international resource sharing arrangements in managing fire in the face of climate change. *Fire* **5**, 88 (2022).
- Matz, C. J. et al. Health impact analysis of PM_{2.5} from wildfire smoke in Canada (2013–2015, 2017–2018). *Sci. Total Environ.* **725**, 138506 (2020).
- Canadian Forest Service, 2022. Canadian Wildland Fire Evacuation Database. Natural Resources Canada, Canadian Forest Service, Northern Forestry Centre, Edmonton, Alberta. Manuscript in preparation. (Accessed 26 April 2022).
- Jain, P., Castellanos-Acuna, D., Coogan, S. C., Abatzoglou, J. T. & Flannigan, M. D. Observed increases in extreme fire weather driven by atmospheric humidity and temperature. *Nat. Clim. Change* **12**, 63–70 (2022).
- Ellis, T. M., Bowman, D. M., Jain, P., Flannigan, M. D. & Williamson, G. J. Global increase in wildfire risk due to climate-driven declines in fuel moisture. *Glob. Change Biol.* **28**, 1544–1559 (2022).
- Francis, J. A. & Vavrus, S. J., Evidence linking Arctic amplification to extreme weather in mid-latitudes. *Geophys. Res. Lett.* **39**, L06801 (2012).
- Francis, J. A. & Vavrus, S. J. Evidence for a wavier jet stream in response to rapid Arctic warming. *Environ. Res. Lett.* **10**, 014005 (2015).
- Mann, M. E. et al. Influence of anthropogenic climate change on planetary wave resonance and extreme weather events. *Sci. Rep.* **7**, 1–12 (2017).
- Blackport, R. & Screen, J. A. Insignificant effect of Arctic amplification on the amplitude of midlatitude atmospheric waves. *Sci. Adv.* **6**, eaay2880 (2020).
- Dai, A. & Song, M. Little influence of Arctic amplification on mid-latitude climate. *Nat. Clim. Change* **10**, 231–237 (2020).
- Abatzoglou, J. T. & Williams, A. P. Impact of anthropogenic climate change on wildfire across western US forests. *Proc. Natl Acad. Sci.* **113**, 11770–11775 (2016).
- Burke, M. et al. The changing risk and burden of wildfire in the United States. *Proc. Natl Acad. Sci.* **118**, e2011048118 (2021).
- Hersbach, H. et al. ERA5 hourly data on pressure levels from 1959 to present. Copernicus Climate Change Service (C3S) Climate Data

- Store (CDS). <https://doi.org/10.24381/cds.bd0915c6> (2018b). (Accessed 20 Sept 2022).
39. Dole, R. M. & Gordon, N. D. Persistent anomalies of the extratropical Northern Hemisphere wintertime circulation: Geographical distribution and regional persistence characteristics. *Mon. Weather Rev.* **111**, 1567–1586 (1983).
40. Miller, R. L., Lackmann, G. M. & Robinson, W. A. A new variable-threshold persistent anomaly index: Northern Hemisphere anomalies in the ERA-Interim reanalysis. *Mon. Weather Rev.* **148**, 43–62 (2020).
41. Renwick, J. A. Persistent positive anomalies in the Southern Hemisphere circulation. *Mon. Weather Rev.* **133**, 977–988 (2005).
42. Gibson, P. B. et al. Ridging associated with drought across the western and southwestern United States: Characteristics, trends, and predictability sources. *J. Clim.* **33**, 2485–2508 (2020).
43. Parsons, S., Renwick, J. A. & McDonald, A. J. An assessment of future Southern Hemisphere blocking using CMIP5 projections from four GCMs. *J. Clim.* **29**, 7599–7611 (2016).
44. Diffenbaugh, N. S. Verification of extreme event attribution: Using out-of-sample observations to assess changes in probabilities of unprecedented events. *Sci. Adv.* **6**, eaay2368 (2020).
45. Swain, D. L., Singh, D., Touma, D. & Diffenbaugh, N. S. Attributing extreme events to climate change: a new frontier in a warming world. *One Earth* **2**, 522–527 (2020).
46. Hall, R. J. et al. Generating annual estimates of forest fire disturbance in Canada: the National Burned Area Composite. *Int. J. Wildland Fire* **29**, 878–891 (2020).
47. Eidenshink, J. et al. A project for monitoring trends in burn severity. *Fire Ecol.* **3**, 3–21 (2007).
48. Van Wagner, C. E. Development and Structure of the Canadian Fire Weather Index System. *Forestry Technical Report Vol. 35* (Canadian Forestry Service Headquarters, Ottawa, 1987).
49. Lawson, B. D. & Armitage, O. B. Weather guide for the Canadian forest fire danger rating system. (Canadian Forest Service, 2008).
50. Sedano, F. & Randerson, J. T. Vapor pressure deficit controls on fire ignition and fire spread in boreal forest ecosystems. *Biogeosciences* **11**, 1309–1353 (2014).
51. Williams, A. P. et al. Correlations between components of the water balance and burned area reveal new insights for predicting forest fire area in the southwest United States. *Int. J. Wildland Fire* **24**, 14–26 (2014).
52. Hersbach, H. et al. ERA5 hourly data on single levels from 1959 to present. Copernicus Climate Change Service (C3S) Climate Data Store (CDS). <https://doi.org/10.24381/cds.adbb2d47> (2018a). (Accessed 20 Sept 2022).
53. Alduchov, O. A. & Eskridge, R. E. Improved Magnus form approximation of saturation vapor pressure. *J. Appl. Meteorol.* **35**, 601–609 (1996).
54. McElhinny, M., Beckers, J. F., Hanes, C., Flannigan, M. & Jain, P. A high-resolution reanalysis of global fire weather from 1979 to 2018—overwintering the Drought Code. *Earth Syst. Sci. Data* **12**, 1823–1833 (2020).
55. Van Wagner, C. E. *A Method of Computing Fine Fuel Moisture Content Throughout the Diurnal Cycle* Information Report PS-X-69 (Canadian Forestry Service, 1977). <https://www.nature.com/articles/s41586-024-07028-5>.
56. De Frenne, P. et al. Forest microclimates and climate change: Importance, drivers and future research agenda. *Glob. Change Biol.* **27**, 2279–2297 (2021).
57. Wang, X. et al. cffdrs: an R package for the Canadian Forest Fire Danger Rating System. *Ecol. Process* **6**, 5 (2017).
58. Magnussen, S. & Taylor, S. W. Inter- and intra-annual profiles of fire regimes in the managed forests of Canada and implications for resource sharing. *Int. J. Wildland Fire* **21**, 328–341 (2012).
59. Hansen, M., Song, X. Vegetation Continuous Fields (VCF) Yearly Global 0.05 Deg [Data set]. NASA EOSDIS Land Processes DAAC. <https://doi.org/10.5067/MEaSUREs/VCF/VCF5KYR.001> (2018). Accessed 8 June 2023.
60. Youssouf, H. et al. Quantifying wildfires exposure for investigating health-related effects. *Atmos. Environ.* **97**, 239–251 (2014).
61. Gupta, P., Remer, L. A., Patadia, F., Levy, R. C. & Christopher, S. A. High-resolution gridded level 3 aerosol optical depth data from modis. *Remote Sensing* **12**, 2847 (2020).
62. Krstic, N. & Henderson, S. B. Use of MODIS data to assess atmospheric aerosol before, during, and after community evacuations related to wildfire smoke. *Remote Sens. Environ.* **166**, 1–7 (2015).
63. Center for International Earth Science Information Network - CIESIN - Columbia University. Gridded Population of the World, Version 4.11 (GPWv4): Population Count, Revision 11. Palisades, NY: NASA Socioeconomic Data and Applications Center (SEDAC). <https://doi.org/10.7927/H4JW8BX5> (2018). (Accessed 5 April 2022).
64. Randles, C. A. et al. The MERRA-2 aerosol reanalysis, 1980 onward. Part I: System description and data assimilation evaluation. *J. Clim.* **30**, 6823–6850 (2017).

Author contributions

P.J. led and designed the study with help from A.R.S., D.A.C., J.T.A. and M.F. P.J. and A.R.S. conducted the upper air (PPA) analysis; P.J. and D.A.C. analyzed fire weather data. P.J. led the writing of the manuscript and all authors read and edited this manuscript.

Competing interests

The authors declare no competing interests.

Additional information

Supplementary information The online version contains supplementary material available at <https://doi.org/10.1038/s43247-024-01346-2>.

Correspondence and requests for materials should be addressed to Piyush Jain.

Peer review information *Communications Earth & Environment* thanks Michael Fromm, Vikki Thompson and the other, anonymous, reviewer(s) for their contribution to the peer review of this work. Primary Handling Editors: Yongqiang Liu, Clare Davis and Aliénor Lavergne.

Reprints and permissions information is available at <http://www.nature.com/reprints>

Publisher's note Springer Nature remains neutral with regard to jurisdictional claims in published maps and institutional affiliations.

Open Access This article is licensed under a Creative Commons Attribution 4.0 International License, which permits use, sharing, adaptation, distribution and reproduction in any medium or format, as long as you give appropriate credit to the original author(s) and the source, provide a link to the Creative Commons licence, and indicate if changes were made. The images or other third party material in this article are included in the article's Creative Commons licence, unless indicated otherwise in a credit line to the material. If material is not included in the article's Creative Commons licence and your intended use is not permitted by statutory regulation or exceeds the permitted use, you will need to obtain permission directly from the copyright holder. To view a copy of this licence, visit <http://creativecommons.org/licenses/by/4.0/>.

© Crown 2024